Unprecedentedly Strong and Narrow Electromagnetic Emissions Stimulated by High-Frequency Radio Waves in the Ionosphere

L. Norin,* T. B. Leyser, E. Nordblad, and B. Thidé
Swedish Institute of Space Physics, Uppsala, Sweden

M. McCarrick
BAE Systems Advanced Technologies, Washington, D.C., USA
(Received 23 October 2008; published 12 February 2009)

Experimental results of secondary electromagnetic radiation, stimulated by high-frequency radio waves irradiating the ionosphere, are reported. We have observed emission peaks, shifted in frequency up to a few tens of Hertz from radio waves transmitted at several megahertz. These emission peaks are by far the strongest spectral features of secondary radiation that have been reported. The emissions are attributed to stimulated Brillouin scattering, long predicted but hitherto never unambiguously identified in high-frequency ionospheric interaction experiments. The experiments were performed at the High-Frequency Active Auroral Research Program (HAARP), Alaska, USA.

DOI: 10.1103/PhysRevLett.102.065003 PACS numbers: 94.20.Tt, 52.25.Os, 52.35.Mw, 94.20.wf

Ionospheric plasma turbulence can be created on demand by the injection of powerful high-frequency (HF) radio waves from ground-based transmitters [1,2]. The HF pumped turbulence emits secondary electromagnetic (EM) radiation that can be detected and measured on the ground [3]. This radiation forms richly structured and highly repeatable sidebands up to hundreds of kilohertz from the transmitted frequency f_0 [4]. The intensity of the sideband radiation rarely exceeds -50 dB relative to the ionospherically reflected pump wave. In this Letter we present results from experiments performed at the High-Frequency Active Auroral Research Program (HAARP), located near Gakona, Alaska, USA. We report sideband emissions of unprecedented strength, reaching up to -10 dB relative to the reflected pump wave. The emissions were shifted by only up to a few tens of Hertz from f_0 and we attribute them to stimulated Brillouin scattering (SBS), i.e., backscattering from stimulated ion acoustic waves. SBS has long been predicted and searched for in ionospheric HF interaction experiments in an overdense ionosphere [5], but such observations have never previously been reported. SBS from an underdense ionosphere has been predicted [6] and observed using VHF radar [7] and, tentatively, using HF radio waves [8].

We present data from 14 different experiments performed 21–26 February 2008 at the HAARP facility (geographical coordinates 62.39° N, 145.15° W). The effective radiated power was 1 GW, which exceeds the capability of all other similar HF facilities. The reflected EM signal was measured using a Hewlett Packard 1437A 23 bit (>100 dB dynamic range) digital baseband signal analysis system connected to a wide band HF antenna. The instantaneous signal bandwidth was 160 kHz. The measurements were performed in Gakona (geographical coordinates 62.30° N, 145.27° W) approximately 11 km to the southwest of HAARP. Local time was UT-9h.

The HF radio waves had *O* mode polarization and the pump beam direction was alternated between vertical (0° azimuth, 90° elevation) and the geomagnetic zenith (MZ), (202° azimuth, 76° elevation). The beam was transmitted in a continuous or quasicontinuous wave mode (for example 30 s on, 30 s off) for up to two hours per experiment. Every minute for the duration of an experiment, between 8 s and 10 s worth of continuous data was captured. The exact pump scheme varied in the different experiments, but in all but one experiment the sideband emissions had reached a steady state when captured. The non-steady-state data set is treated separately. The recorded time series were analyzed by applying a fast Fourier transform with a Hanning window, corresponding to 0.8 s, revealing sideband emissions in the frequency domain with a resolution of 1.25 Hz.

In Fig. 1 we show frequency spectra from 13 different experiments with $2.7 \leq f_0 \leq 4.5$ MHz, corresponding to a range from below the second harmonic of the ionospheric electron gyrofrequency to above the third harmonic. In six of the experiments the beam was directed vertically [Fig. 1(a)], in the other seven towards the MZ [Fig. 1(b)]. In the spectra the reflected pump wave at f_0 is seen as a dc component and narrow emission peaks appear both up- and downshifted from f_0. In the following we refer to these emissions as ''narrow peaks'' (NPs). In all experiments the NPs were asymmetric in power, and in all but one experiment the downshifted NP was stronger than the upshifted NP.

In Fig. 1(a) (vertical beam) we see that the NPs appear symmetrically around f_0 and that their frequency shifts Δf from f_0 increase slightly with increasing f_0. For $f_0 = 3.3$ MHz, $\Delta f = \pm(23\text{–}25)$ Hz whereas for $f_0 = 4.5$ MHz, $\Delta f = \pm(26\text{–}30)$ Hz. The NPs reach up to -40 dB relative to the reflected pump wave and up to 30 dB relative to the background noise level.

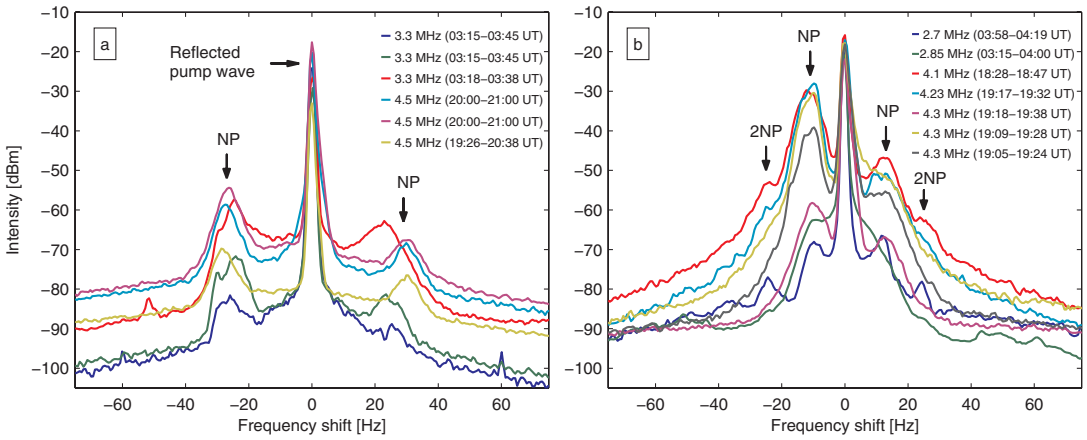

FIG. 1 (color online). Frequency spectra of radio emissions revealing narrow peaks (NPs) for different f_0. The pump beam was transmitted vertically (a) and toward geomagnetic zenith (b). A weak interference due to the power net can be seen at $f_0 \pm 60$ Hz and -95 dBm in (a). Note the second set of peaks (2NPs) at approximately $f_0 \pm 25$ Hz in (b).

In Fig. 1(b) (MZ beam) the downshifted NP is well developed in most spectra but the upshifted NP cannot always be identified. The maximum intensity of the NPs, shifted by $\Delta f = \pm(9\text{–}12)$ Hz, is significantly larger than for vertical beams. The strongest NP reaches up to -10 dB relative to the reflected pump wave and up to 65 dB relative to the background noise level. This is by far the strongest sideband emission reported. In some spectra we can also see a weaker second set of NPs (2NPs) with frequency shifts $\Delta f = \pm(24\text{–}26)$ Hz. The 2NPs are $-(10\text{–}30)$ dB relative to the NPs. It is notable that these unprecedently strong EM emissions were obtained during the daytime for a pump beam in the MZ direction. Previously, pumping in the MZ direction has given maximum optical emission intensity [9,10] as well as other heating effects [11], albeit during nighttime conditions. Particularly, optical emissions from MZ beams are 1 order of magnitude larger than in any other beam direction [9].

The NP emissions originate from the ionospheric plasma and are excited by the injected pump wave. No evidence of emissions resembling the NPs could be seen from the transmitted signal, as observed from the output spectrum of the HAARP transmitters and the off-air spectrum from a nearby vertical whip antenna (which sees the ground wave but not the reflected sky wave).

One of the experiments with the pump beam directed towards the MZ at $f_0 = 2.85$ MHz showed an interesting temporal development. The experiment lasted for 107 min and the pump was cycled 2 min on/2 min off. A spectrogram of the EM emissions is shown in the top panel of Fig. 2 together with the critical frequency f_{crit} (the maximum plasma frequency in the ionosphere), the maximum upper hybrid frequency, and the intensity of the reflected pump signal in the bottom panel. The maximum upper hybrid frequency is given by $f_{\text{UH}} = \sqrt{f_{\text{crit}}^2 + f_e^2}$, where we have assumed an electron gyrofrequency $f_e = 1.4$ MHz. At first strong emissions were concentrated within $f_0 \pm 15$ Hz with a maximum intensity at $\Delta f \approx -9$ Hz. The downshifted NP existed, but was not well defined, and the upshifted NP could not be resolved from the continuum. These emissions disappeared after approximately 65 min. At 70 min the NPs appeared again, but weaker in intensity and with larger Δf, starting at $\Delta f \approx \pm 20$ Hz and increasing to $\Delta f \approx \pm 25$ Hz at 95 min after which the NPs vanished. Ionograms provided by the HAARP ionosonde show that initially $f_{\text{crit}} > f_0$ and after 65 min $f_{\text{crit}} < f_0$. At this time the emissions within $f_0 \pm 15$ Hz disappeared and NPs with larger Δf appeared. After approximately 90 min f_{UH} also dropped below f_0, close to the time when the NPs disappeared.

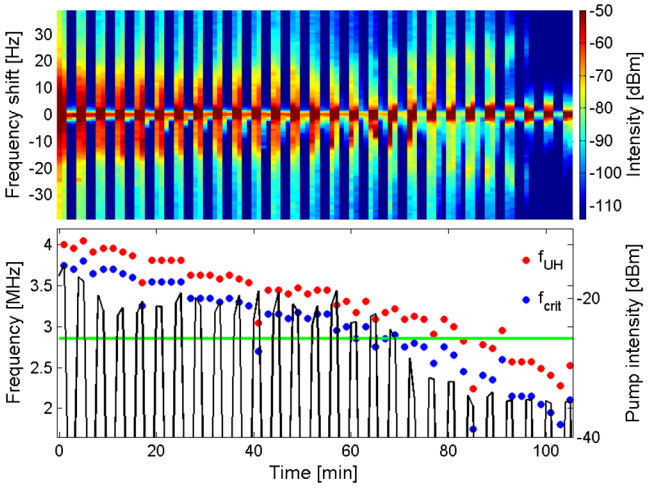

FIG. 2 (color online). Pump beam transmitted towards geomagnetic zenith at $f_0 = 2.85$ MHz (03:15–04:22 UT, 24 February 2008). The pump was cycled 2 min on/2 min off. Top: Spectrogram of received radio emissions, centered on f_0. Bottom: Blue (dark gray) markers show f_{crit}, measured by the HAARP ionosonde. Red (medium gray) markers correspond to $f_{\text{UH}} = \sqrt{f_{\text{crit}}^2 + f_e^2}$, and the green (light gray) horizontal line indicates f_0. The black line shows the intensity of the reflected signal, with the ordinate to the right.

Figure 3 shows results from the growth phase of the NP emissions following the onset of the radio transmitters. The beam was directed vertically at $f_0 = 4.5$ MHz and the transmitters were cycled 30 s on, 30 s off. Figure 3(a) shows a spectrogram of the sideband emissions. At time $t = 0$ the reflected sky wave was received, resulting in a broadening of the Fourier transform seen as a wide, vertical line. The NPs appear at $\Delta f \approx \pm 24$ Hz after less than a second, reaching a steady state within two seconds. Figure 3(b) displays a steady-state frequency spectrum, obtained as a mean for $4 < t < 8$ s, that clearly shows the NPs. Self-normalizing the intensity of the pump and the two NPs reveal their dynamics, shown in Fig. 3(c), where the downshifted NP reaches a steady-state after approximately one second and the weaker upshifted NP after about two seconds. In Fig. 3(d) we show the absolute intensities of the NPs during the first 2.5 s after pump turn-on and we see that the up- and downshifted NPs have approximately the same growth rate, $\gamma \approx 8\ \mathrm{s}^{-1}$.

After the growth phase the NPs become stationary and thus they cannot be attributed to transient phenomena, such as relaxation oscillations of the reflection layer or modification of the plasma density profile [12]. Further, in all experiments the downshifted NP was more intense than the upshifted NP, except for the one weakest case in Fig. 1(b). Particularly, the stronger the NPs, the stronger the asymmetry is between the up- and downshifted peaks. Such an asymmetry is in agreement with predictions from stimulated scattering theory. Since Alfvén waves have

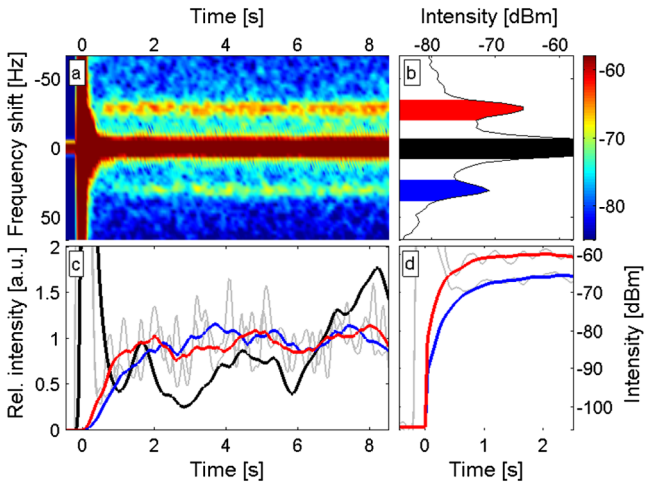

FIG. 3 (color online). Transient stage of wave interaction, vertical pump beam at $f_0 = 4.5$ MHz (20:26:00–20:38:30 UT, 26 February 2008). Panel (a) shows a spectrogram of the received signal. A colorbar displaying the intensity in dBm is located to the far right. In panel (b) the stationary frequency spectrum is shown and in panel (c) the smoothed, relative intensities of the pump wave (black), the downshifted NP [red (medium gray)] and the upshifted NP [blue (dark gray)] are shown. In panel (d) the smoothed, absolute intensities of the downshifted NP [red (medium gray)] and the upshifted NP [blue (dark gray)] are shown for time $-0.5 < t < 2.5$ s. Original intensities are depicted by thin light gray lines.

wavelengths that are too long at the observed Δf we suggest that the observed NPs are the results of SBS, in which the transmitted radio wave interacts with an ion acoustic wave. In order to simplify the analysis, we assume that the observations originate from a pure backscattering process as the observation point was located much closer to the transmitter ($\approx$11 km) than the ionospheric interaction region ($\approx$200 km).

For efficient scattering to occur two matching conditions on the angular frequencies ω and wave vectors $\vec{k}$ must be fulfilled,

$$\omega_0 = \omega_1 \pm \omega_a, \tag{1}$$

$$\vec{k}_0 = \vec{k}_1 \pm \vec{k}_a. \tag{2}$$

Subscripts 0 and 1 denote EM and a denotes an ion acoustic wave. Because of the great difference in phase velocity of the EM and ion acoustic wave, Eq. (2) reduces to $k_a \approx 2k_0$.

Ion acoustic waves exist naturally in the ionosphere but are heavily Landau damped for similar electron and ion temperatures, $T_e \approx T_i$. However, for the high pump duty cycles used in the experiments it is expected that $T_e/T_i > 1$, leading to a decrease in the Landau damping. An analytical expression for the dispersion relation of an ion acoustic wave, propagating with an angle θ to the ambient magnetic field is given by [13]

$$\omega_a = \frac{k_a c_a \cos\theta}{\sqrt{1 + k_a^2 \rho_i^2}}, \tag{3}$$

where c_a denotes the ion acoustic speed and $\rho_i = c_a/\omega_{\mathrm{ci}}$, where ω_{ci} is the ion gyrofrequency. Near the interaction region the ion population is dominated by atomic oxygen and $\omega_{\mathrm{ci}} \approx 2\pi \times 47\ \mathrm{s}^{-1}$.

At low altitudes, where the change in wave number of the EM wave is negligible, the EM wave can be described by the vacuum dispersion relation, $\omega_0 = k_v c$, where c is the vacuum light speed. The vacuum wave number, k_v, is an upper limit for k_0 since in the plasma $k_0 < k_v$. We can, using Eqs. (1)–(3), find a lower limit on c_a for a given ω_a. Using $\omega_a = 2\pi\Delta f$ from the experiments with the pump beam directed vertically we find that the lower limit is $c_a = 1.3(0.1)$ km/s.

Figure 4(a) shows a ray tracing for a vertical ray, for which the O mode is reflected at $\omega_p = \omega_0$, where ω_p is the plasma frequency. Equation (2) can be satisfied at any altitude below the reflection height but the largest growth rate is expected to occur where dk_0/dz is small so that the convective damping of SBS is limited. In Fig. 4(a), c_a is shown at different altitudes such that the observed Δf is consistent with the matching conditions (1) and (2). Below the upper hybrid resonance height the convective damping is small and $c_a \lesssim 2$ km/s. For interaction at higher altitudes, c_a must be larger to be consistent with the observations.

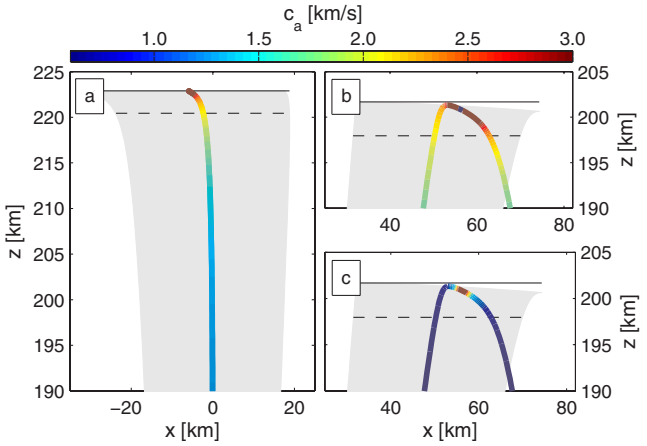

FIG. 4 (color online). Ray tracings from $x = 0$ for a vertical beam with $f_0 = 4.5$ MHz (a) and a MZ beam with $f_0 = 2.7$ MHz (b),(c). In (a) the colored line shows c_a for which the observed frequency shifts $\Delta f = \pm 28$ Hz of the NPs are consistent with SBS. For the MZ beam there are two sets of NPs. In (b) the shown c_a corresponds to $\Delta f = \pm 24$ Hz and in (c) the c_a corresponds to $\Delta f = \pm 9$ Hz. The beam width (10°) is shown by shaded areas. The horizontal, solid lines indicate $\omega_p = \omega_0$ and the dashed lines $\omega_p = \sqrt{\omega_0^2 - \omega_e^2}$.

As seen in Figs. 4(b) and 4(c), a wave transmitted towards the MZ will refract from the transmission angle as it approaches the reflection height. There are two regions in which dk_0/dz is small: below the upper hybrid resonance height and close to the reflection height. It is interesting that for $f_0 = 2.7$ MHz, the weakest case in Fig. 1(b), the NPs at $\Delta f \approx \pm 9$ Hz and the 2NPs at $\Delta f \approx \pm 24$ Hz can be seen. The NPs have Δf similar to those of the strongest NPs in Fig. 1(b). The 2NPs have Δf similar to the NPs observed for vertical beams in Fig. 1(a). In Fig. 4(b) we show c_a at different altitudes such that Δf of the 2NPs are consistent with SBS. The corresponding case for the NPs is shown in Fig. 4(c). It is seen in Fig. 4(b) that below the upper hybrid resonance height the required $c_a \lesssim 2$ km/s. For the same c_a there exists an interaction region near the reflection height in Fig. 4(c) where the matching conditions can be fulfilled. In both of these two regions dk_0/dz is small, so that the NPs and the 2NPs can be created simultaneously for similar c_a but at different altitudes.

The strongest NPs, excited near the reflection height and only $-(10$–$15)$ dB weaker than the reflected pump wave, occur simultaneously with more intense sets of 2NPs [see Fig. 1(b)]. These 2NPs could be the result of a cascade in the SBS, suggested by the asymmetric continuumlike flanks compared to the case in Fig. 1(a) where the NPs have much sharper cutoffs at the largest shifts from f_0. Independent, simultaneous measurements of c_a, for example, by incoherent scatter radar, would allow for finding the interaction altitudes as well as to decide which is the dominant generation process for the 2NP. For future work it would also be interesting to investigate the dependence of the NPs on the radiated power and to estimate how large the ion acoustic waves must be in order to generate the observed NPs.

The sudden change in Δf of the NPs, at 65 min in Fig. 2, coincides with the time the EM wave is able to propagate through the ionosphere, $f_0 \gtrsim f_{\mathrm{crit}}$, thereby suddenly increasing the smallest possible value of $|k|$ and simultaneously increasing θ. This leads to scattering from ion acoustic waves with larger ω_a [see Eq. (3)], consistent with the observations. Furthermore, for $f_0 \gtrsim f_{\mathrm{UH}}$ the heating of the electrons in the ionosphere decreases significantly and, thus, the Landau damping of the ion acoustic waves increases. This is consistent with the NPs vanishing in Fig. 2 after 95 min. The importance of pump-induced slowly growing electron heating for the SBS to occur is also consistent with the slow growth of the NP emissions seen in Fig. 3.

We gratefully acknowledge Björn Gustavsson, Mike Kosch, Gennady Milikh, and Todd Pedersen for additional experimental data; Lennart Åhlén, Paul Bernhardt, Craig Selcher and the staff of the HAARP facility for technical support. We also thank a referee for useful comments. This work was supported financially by the Göransson-Sandviken foundation and the Swedish Research Council.

*Also at Department of Physics and Astronomy, Uppsala University, Sweden. lars.norin@irfu.se

[1] T. R. Robinson, Phys. Rep. **179**, 79 (1989).
[2] A. V. Gurevich, Phys. Usp. **50**, 1091 (2007).
[3] B. Thidé, H. Kopka, and P. Stubbe, Phys. Rev. Lett. **49**, 1561 (1982).
[4] T. B. Leyser, Space Sci. Rev. **98**, 223 (2001).
[5] L. Stenflo, EOS Trans. Am. Geophys. Union **60**, 595 (1979).
[6] K. B. Dysthe, E. Leer, and J. Trulsen, J. Geophys. Res. **82**, 717 (1977).
[7] J. A. Fejer, K. Rinnert, and R. Woodman, J. Geophys. Res. **83**, 2133 (1978).
[8] B. Thidé, H. Derblom, Å. Hedberg, H. Kopka, and P. Stubbe, Radio Sci. **18**, 851 (1983).
[9] T. R. Pedersen, M. McCarrick, E. Gerken, C. Selcher, D. Sentman, H. C. Carlson, and A. Gurevich, Geophys. Res. Lett. **30**, 1169 (2003).
[10] M. J. Kosch, T. Pedersen, E. Mishin, M. Starks, E. Gerken-Kendall, D. Sentman, S. Oyama, and B. Watkins, J. Geophys. Res. **112**, A08304 (2007).
[11] M. T. Rietveld, M. J. Kosch, N. F. Blagoveshchenskaya, V. A. Kornienko, T. B. Leyser, and T. K. Yeoman, J. Geophys. Res. **108**, 1141 (2003).
[12] L. A. Lobachevsky, Y. V. Gruzdev, V. Y. Kim, G. A. Mikhaylova, V. A. Panchenko, V. P. Polimatidi, V. A. Puchkov, V. V. Vaskov, P. Stubbe, and H. Kopka, J. Atmos. Terr. Phys. **54**, 75 (1992).
[13] D. G. Swanson, *Plasma Waves* (Institute of Physics Publishing, Bristol, 2003), 2nd ed..